INTERNATIONAL JOURNAL OF
AUTOMOTIVE SCIENCE AND TECHNOLOGY

2022, VOL. 6, NO:4, 364-378
www.ijastech.org
e-ISSN: 2587-0963

Investigation on Different Driving Cycles and Scenarios Considering the Autonomous Electric Vehicles

Uğur Demir[1*] and Zeliha Kamış Kocabıçak[2]

0000-0001-7557-3637, 0000-0003-3292-8324

[1] *Mechatronics Engineering Department, Faculty of Technology, Marmara University, Istanbul, 34854, Turkey*
[2] *Automotive Engineering Department, Engineering Faculty, Bursa Uludağ University, Bursa, 16059, Turkey*

Abstract

This study presents a series of analyzes considering the traction and steering demands of an autonomous electric vehicle (AEV) as a shuttle. The considered analyzes in here are dealt with as driving cycle (DC) and driving scenarios (DS) to assess the traction and steering performance of the AEV. The aim of this study is to evaluate the issues such as over engineering for AEV traction and steering motor requirements on a certain route by comparatively analyzing traditional and dynamic calculation under the DC and DS. Therefore, DC and DS in the literature are evaluated in terms of different applications, optimization techniques, generation algorithm, parametric characterization, e-motor type etc. Afterwards, NEDC, US06, WLTC, Double Lane Change (DLC), Constant Radius (CR) and Slowly Increase Steer (SIS) are determined. Then, they are arranged according to the vehicle-specific limits on an electric golf car. The modified DCs and DSs are run on the dynamic model of the vehicle. In the performed analysis, the parameters such as reference trajectory tracking, yaw angle, tractive and steering forces, lateral and longitudinal displacement-acceleration, steering and traction motor power–speed-torque are investigated. Then the obtained results are evaluated by comparing the traditional calculation results.

Keywords: Driving cycle; Driving Scenario; Autonomous Vehicle; Steering and Traction Dynamics.

Research Article

https://doi.org/10.30939/ijastech..1178321

Received 21.09.2022
Revised 09.11.2022
Accepted 10.11.2022

* Corresponding author
Uğur Demir
udemir@marmara.edu.tr
Address: Mechatronics Engineering Department, Faculty of Technology, Marmara University, Istanbul, Turkey
Tel:+903122028653

1. Introduction

In recent years, interest in emission reduction, clean energy and renewable energy sources has been increasing rapidly. This situation has also accelerated the work on electric vehicles. Especially in the last 20 years, energy efficiency issues have been focused on to increase the range of electric vehicles [1,2]. Energy efficiency basically focuses on alternative battery types, battery management, power electronics drives and electric traction units [3,4].

On the other hand, driving assistants, which have become mandatory to be used with the regulations coming to today's commercial and passenger vehicle concepts, attract a great deal of attention. Driving assistant technologies such as lane tracking, emergency braking and pedestrian detection, and speed limit warnings make it possible to increase the driving safety of passengers and drivers [5]. By the development of driving assistant technology, the interest of the unmanned autonomous vehicle technologies is increased rapidly. Today, vehicles with internal combustion engines, hybrid vehicles and electric vehicles have many driving assistant technologies. In particular, it is seen that some electric vehicle manufacturers focus their efforts on making their vehicles autonomous, that is, they invest in developing fully autonomous electric vehicles. Considering the autonomous vehicle, especially autonomous electric vehicles, the basic work is concentrated on the control of the lateral and longitudinal vehicle dynamics [6]. As longitudinal vehicle dynamics basically controls the acceleration and braking demands of the vehicle, it can already be evaluated in the same concept as normal electric vehicles. On the other hand, the lateral vehicle dynamics control tries to meet the demands on the steering of the vehicle. Thus, the steering with the electric motor stands out in autonomous vehicles [7].

Therefore, the development of the electric motor drive units for traction and steering, especially in autonomous electric vehicles, directly affects driving performance and safety and the use of energy resources.

Design and optimization studies on electric motors on electric vehicles are mostly subject to component-based verification processes. In recent years, optimization studies for electric vehicles both component-based and system-based have shown that electric traction motors improve design [8,9].

On the other hand, the studies related to autonomous vehicles mostly deal with issues such as path tracking, path following, path planning, sensor fusion and improved sensing [10]. In the literature, it has been seen that some steering with e-motor studies are component-based within the scope of driving support [11].

The obtained data from the literature review show the driving performance of traction and steering motors on autonomous electric vehicles (maneuverability, acceleration and braking, battery consumption performance, reference trajectory tracking, etc.), in different driving cycles (ECE R15, NEDC, EUDC, FTP75, etc.). US06 etc.) [12] and different control methods (Pure Pursuit, Model Predictive Control and Stanley etc.) [13] for path tracking could not find any studies on system-based validation.

It is obvious that suitable and optimal electric motors will directly affect the traction and steering dynamics, increase driving performance and driving safety, and increase autonomous driving sensitivity. In this study, it is planned to evaluate an autonomous electric vehicle on the power demand needed in different driving cycles and scenarios. The contribution of this study to the literature is to analyze traction and steering demands, to identify potential opportunities and to prevent overengineering.

2. Driving Cycles and Scenarios

Many studies have been done on the driving cycle in the literature. Studies on the driving cycle can be grouped into two categories. These are studies for derivation/generation of driving cycles [14-43] and studies for analysis and optimization of element such as vehicle or component performance under driving cycles [44-74].

The studies on deriving the driving cycle [14-43]; the discussed driving cycles can be evaluated in terms of vehicle types, techniques used and the analyzed parameters. These are given in Tables 1-4.

Table 1. Driving Cycles in [14-43]

Artemis 150	Cyc-US06	FTP-75
Brunswick-cycle	Cyc-US06-HWY	HHDD-Cycle-Creep-Mode
Cyc-ARB02	Cyc-VAIL2NREL	HHDDT-Cycle-Cruise-Mode
Cyc-BUSRTE	Cyc-WVUCITY	HHDDT-Cycle-Transient-Mode
Cyc-CLEVELAND	Cyc-WVUINTER	HWY
Cyc-CSHVR-Vehicle	Cyc-WVUSUB	heavy-duty highspeed cycle
Cyc-HL07	CTBDS_UD	heavy-duty cycle in suburb
Cyc-HWFET-MTN	CWTVC	heavy-duty interpolation cycle in urban
Cyc-IM240	California-Unified-Cycle	JC08
Cyc-india-hwy-sample	City-Suburban-Heavy-Vehicle-Cycle	JE05
Cyc-india-urban-sample	Chinese typical city	Japan 10-15
Cyc-NREL2VAIL	Beijing-cycle	Magny-Cours racing circuit
Cyc-NurembergR36	Changchun-cycle	Manhattan-test-cycle
Cyc-NYCC	Dalian	New-York-Composite-Cycle
Cyc-NYCCOMP	Guangzhou Driving Cycle	New-York-Bus-cycle
Cyc-NYCTRUCK	Shangai Driving Cycle	Orange-County-Bus-Cycle
Cyc-REP05	Tianjin (Congested, highway, mixture)	SC03-Supplemental-FTP
Cyc-SC03	Zhuzhou	stop-and-go cycle
Cyc-UDDS	ECE 15	UDDS
Cyc-UDDSHDV	EPA-Highway-Fuel-Economy-Cycle	US06-Supplemental-FTP
Cyc-UKBUS6	EPA-New-York-City-Cycle	WLTC
Cyc-UKBUS-MASS-VAR1	FIGE-cycle	WLTC class 3
Cyc-UNIF01	FTP-72	WLTP

Table 2. Vehicle Types in [14-43]

EV	HEV	PHEV	Bus	Truck	Racing Car	Passenger	Test Bench HIL

Table 3. Driving Cycle Generation Techniques in [14-43]

Genetic Algorithm (GA)	Energy Cycle Model with Stochastic and Deterministic Inputs
SOM Neural Network (Self Organized Mapping)	Stochastic and Deterministic Analyses, Probability Density Function Generation
Genetic Agency, SVM(Support Vector Machine)	Markov Chain Process, Micro Segmentation
Neuro-Fuzzy Hybrid Algorithm	Improved Hierarchical Clustering Algorithm, SVM (Support Vector Machine)
Microstrip Statical Analyses	Microstrip Segment., Markov Chains, Statical-Spectral-Time Domain Analyses
SOM Neural Network (Self Organized Mapping)	Stochastic Model and Clustering Analyses
Map Based Linear Estimation Strategy	LVQ, DCI model (Driving Cycle Identification)
Markov Chain Process (MC)	Statical Normal Distribution of Velocity and Acceleration
Microstrip Analyses	Markov Chain, GA to hybrid MCE (Markov Chain Evaluation) Algorithm
Journey Mapping	Markov Chain Process, Stochastic Dynamic Programming
Markov Chain Process, State Code Method	Driving Behavior Based Optimization
Annealing Optimization Algorithm	Conditional Probabilities of Acceleration Based on Logistic Regression Models
Fuzzy Logic, LVQ(Learning Vector Quantization)	Parameter Space Based Micro Strip Segment., Clustering, Classification MC
K-Means Clustering Method	GA, MC, Low Frequency Interpolation, K-Means Clustering

Table 4. Parametric Characterization of the Driving Cycles in [14-43]

Look Ahead Distance	Correlative degree of VA distribution (%)	Ratio of speed between 0 to 10 km/h (%)
Real Driving Emission	Percent of time idling (%) and Time (s)	Ratio of speed between 10 to 20 km/h (%)
Driver Aggressiveness	Percent of time cruising (%) and Time (s)	Ratio of speed between 20 to 30 km/h (%)
Route Recognition	Percent of time acc. (%) and Time (s)	Ratio of speed between 30 to 40 km/h (%)
Drive Cycle	Percent of time decel. (%) and Time (s)	Ratio of speed between 40 to 50 km/h (%)
Duty Cycle	Travel time / Duration (s)	Ratio of speed between 50 to 60 km/h (%)
Driving Pattern	Travel distance / Cycle length (m)	Ratio of speed between 60 to 70 km/h (%)
Driving Profile	Average / Mean Velocity / Speed (m/s)	Ratio of speed between 70 to 80 km/h (%)
Driving Pulse	Average / Mean Acceleration (m/s^2)	Ratio of speed >80km/h (%)
Stops per km (s)	Average / Mean Deceleration (m/s^2)	% of time in speed inter. 0 to 5 m/s(%)
Stop Times	Maximum Velocity / Speed (m/s)	% of time in speed inter. 5 to 10 m/s(%)
Longest Stop (s)	Maximum Acceleration (m/s^2)	% of time in speed inter. 10 to 15 m/s(%)
Gradual braking	Maximum Deceleration (m/s^2)	% of time in speed interval > 15 m/s (%)
Mean Slope (%)	Minimum Velocity / Speed (m/s)	% of time in Acc. Inter. 0 to 7 m/s^2 (%)
Standard Deviation Slope (%)	Minimum Acceleration (m/s^2)	% of time in Acc. interval >7 m/s^2 (%)
Maximal Slope (%)	Minimum Deceleration (m/s^2)	% of time in Decel. Inter. -7 to 0 m/s^2(%)
Minimal Slope (%)	Standard Deviation Velocity / Speed (m/s)	% of time in Decel. interval <-7 m/s^2 (%)
Slope / Road Slope (%)	Standard Deviation Acceleration (m/s^2)	Acceleration >0.1m/s^2 Urban (0-60 km/h)
Cold Start Stop Times (s)	Standard Deviation Deceleration (m/s^2)	Acceleration >0.1m/s^2 Rural (60–90 km/h)
Cold Start Average Velocity (m/s)	Mean velocity during accelerating (km/h)	Acc. >0.1m/s^2 Motorway (90-160 km/h)
Cold Start Maximum Velocity (m/s)	Mean velocity during decelerating (km/h)	RPA (Relative Positive Acceleration) Urban (0-60 km/h)
Low Speed Phase (s)	Average Cruising Speed (m/s)	RPA Rural (60–90 km/h)
High Speed Phase (s)	Average Velocity Urban (m/s)	RPA Motorway (90-160 km/h)
Traffic Congestion Level	VA Distribution Correlation Coefficient	Time above 145km/h (s)
Weather Condition	Running speed (except idle speed) (m/s)	Time above 100km/h (s)
Kinetic Energy unit distance (J/m)	Standard Deviation of Driving Speed (m/s)	Highway time ratio (%)
Kinematic Sequence of Velocity (m/s)	Positive Acc. Kinetic Energy Change (W)	Medium speed time ratio (%)
Mean Tractive Force (N)	Mean Positive Velocity (m/s)	Low speed time ratio (%)
Road Type, Condition, Topography,	Mean Positive Acceleration (m/s^2)	Velocity Noise (Amp., Frequency, Phase)
Average Climbing (s)	Mean Negative Acceleration (m/s^2)	Mean Power and Energy Need
Average Downhill (s)	Relative Positive Acceleration (m/s^2)	Mean Power and Maximum Power
Average Driving Speed (m/s)	Speed Acceleration Frequency Distribution	Driver Action Analysis (Throttle, Brake)
Vehicle Motion (Turn, Stop-n-Go, Acceleration (Acc), Deceleration(Decel)	Driver Behavior and Habits (Age, Experience, Mood, Reflex Time)	Driving Scenario (Stop-n-Go, Urban, Suburban, Rural, Highway)
Acceleration dependency on speed/gear	Speed variation in free driving	Speed adaptation to the road curvature

The studies for the analysis and optimization of elements such as vehicle or component performance under driving cycles [44-74]; The discussed driving cycles, the techniques used, the considered motor types, the objective function and the analyzed parameters can be evaluated. These are given in Tables 5-9.

Table 5. Driving Cycles in [44-74]

NEDC	NEFZ	Chinese Driving Duty Cycle	Zhuzhou city cycle
J1015	FTP-75	ECE_EUDC Driving Cycle	LUUDC (Loughborough University Urban Drive Cycle)
US06	ARTEMIS	NEDC/Artemis Combined	UDDS (Urban Dynamometer Driving Schedule)
HWFET	jc08	Beijing (China)	US06 (Supplemental Federal Test Procedure/SFTP)
EUDC	FTP72(75)	Karlsruhe (Germany)	Napples Urban Pattern
ECE 15	UC(LA92)	AUDC (Artemis Urban DC)	AEDC (the average efficiency over a driving cycle)
FTP	CADC	NYCC	Bangkok Driving Cycle
WLTC	UNECE R101	HWFET	WHVC
SC03	HWY	REP05	SAEJ227

Table 6. E-Motor Types in [44-74]

PMSM	IPM	Permanent Magnet Assisted Synchronous Reluctance (PMASR)	Induction Motor
IPMSM	SRM	Surface-mounted permanent magnet synchronous motor (SPMSM)	

Table 7. E-Motor Optimization Techniques under Driving Cycles in [44-74]

Frequency Cubic	Central composite design (CCD)	PSO (particle swarm optimization)
Genetic algorithm (GA)	Sequential Surrogate Optimizer (SSO)	Multi-objective design optimization
Taguchi Robust	Differential Evolution Algorithm	Multi-objective genetic algorithm (MOGA)
Bi-Objective Optimization	Sequential quadratic program (SQP)	Multiobjective sequential optimization method (MSOM)
Base point optimization	Loss-minimization algorithm	Root-mean-square error (RMSE)
Kriging model using NSGA II	Machine-based minimization algorithms	Non-dominated sorting genetic algorithm II (NSGA-II)
System-based minimization		

Table 8. Objective Functions in [44-74]

Traction e-motor optimization	Performing electric motor design optimization under driving cycle
Analyzing driving cycles in vehicle design	Analysis of thermal damages in power-drives under driving cycles
Investigation of energy efficiency of electric motor design parameters on driving cycles	Investigation of motor design optimization on temperature-related estimation on life cycles
Investigation of effects on electric motor core materials under driving cycles	Determining the relationship between motor design parameters and driving cycle and analysis of fuel economy
Electric motor design optimization and cooling unit design under thermal load	Effect of motor thermal change on performance and energy consumption
Investigation of the differences between real world driving cycles and standard driving cycles	Analysis of differences in real time driving cycles between Beijing (China) and Karlsruhe (Germany)
Analysis of the effect on emissions	An algorithm study to minimize system-level power-driver losses
Powertrain and fuel consumption improvement	Analyzing motor loss patterns under driving cycles
Analysis of real time optimum torque distribution strategy under driving cycle	Performance analysis of fuel efficiency under driving cycles
Analysis of the performance of powertrain topologies under driving cycles	Investigation of the optimal driving cycle for designing a high-performance hybrid powertrain

Table 9. E-Motor Parametric Analysis under Driving Cycles in [44-74]

Average Vehicle Trip Speed	Copper Loss	Battery Energy/Distance
State of Charge	Driving Cycle Regimes (Highway, Suburban, Urban)	Damage - Distance to Failure
Efficiency	Power Consumption	Heat Generation Rate
Core loss	Fuel Consumption	Power Loss
Temperature	Fuel Saving Ratio	Power Delivered
Flux Density	Rotor Flux	Starting
Peak Power	Cumulative Energy Loss	Acceleration
Rated Power	Drive Loss	Climbing
Peak Torque	Inverter Loss	High Speed
Fuel Economy Improve Rate	Filter Loss	Normal Cruise
Torque-Speed Map	Traction Power	High Torque
CO^2 Nitrogen Emission	Power Range	Low Torque Ripple
Thermal Model	MTPA Trajectory	Strong Fault Tolerance
Lifetime Model	MTPV Trajectory	Wide Speed Range
Hot Spot Temperature	Base Speed	High Efficiency
Torque-Speed Loss Map	Overload Capability	Star or Climbing
Energy-Torque-speed Map	Mechanical Energy	Normal Operation
Iron Loss	Low-Middle-High Speed	Open-Circuit Fault
Id-Iq Currents / D-Q axis	Wheel Energy/Distance	Start-circuit Fault
Winding Temperature	Brake Event / Acceleration Event	High Speed Operation

Basically, the driving cycle consists of 4 main components. These are acceleration, deceleration, idle and cruise. Driving cycles are obtained by arranging these components sequentially to form a cycle. An example for drive cycle components is shown in Figure 1 and it is used for various purposes to analyze the elements such as emission and battery consumption. In the studies conducted between [14-74], the vehicle development processes both component-based analysis of driving cycles and system-level analysis studies are focused. These driving cycles are previously used for vehicles with internal combustion engines. With the widespread use of electric and hybrid vehicles, it has started to be used in basic performance tests here.

One of the main problems in the driving cycle is that the uphill and downhill tests cannot be observed, so it is tried to analyze the sudden acceleration and deceleration components in the driving cycles, although not fully, the effects of these factors. In addition, there are some analysis studies in the literature [75], which are designed in ECE R15, for the downhill and climbing analysis. A driving cycle with slope scenario is given in Figure 2.

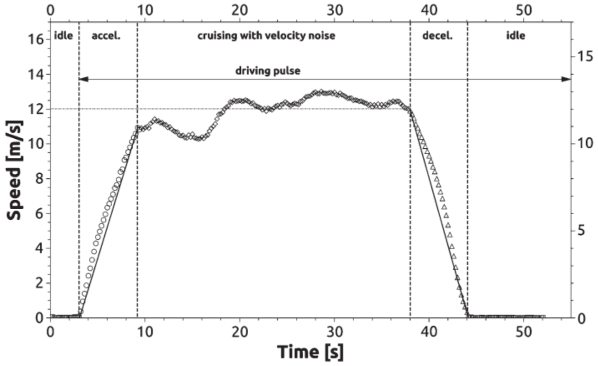

(a) Driving Pulse

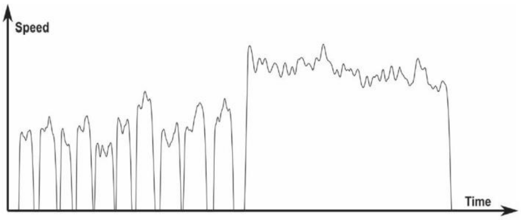

(b) Driving Cycle

Fig 1. Driving Pulse and Driving Cycle Pattern [23]

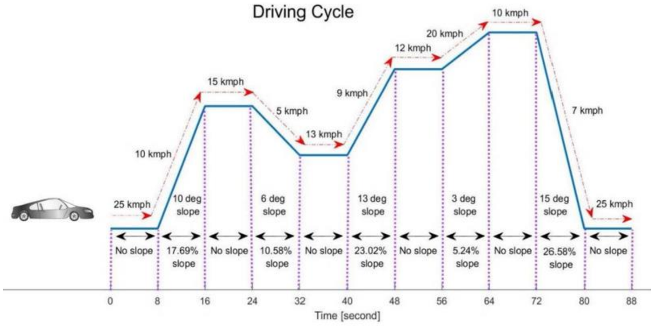

Fig 2. Driving Cycle with Slope Pattern [75]

On the other hand, with the development of driving assistant and autonomous vehicle technologies, driving scenarios are also needed for testing and analysis. Especially when autonomous electric vehicles are considered, driving cycles or driving scenarios including test maneuvers are needed.

The observed standards from the literature [76];

- Swedish Standards Institute containing ISO standards
- SAE International Digital Library
- FMVSS, Federal Motor Vehicle Safety Standards (Sine with dwell FMVSS216)
- EuroNCAP (information regarding ESC standard)
- NHTSA (information regarding ESC standard)
- ISO/TC 22 Road vehicles (Relevant parts regarding passenger cars.)
- Motor sport magazines (e.g. Acceleration 0 - 100 km/h)

To evaluate the most useful test maneuvers for a vehicle-based study, the tests that can be used to validate a real vehicle behavior and the tests that can be used to validate a vehicle model and demonstrate model limitations are listed as follows [76];

- Steady state cornering ISO 4138
- Sine with dwell FMVSS126 S7.9
- Fishhook NHTSA (FEO05)
- Sine steer increased amplitude (FEO05)
- Double lane change ISO 3888-1
- Sinusoidal input, one period ISO 7401 (ISO 8725)
- Obstacle avoidance ISO 3888-2
- Step input ISO 7401
- Pulse input ISO 7401
- Random input ISO 7401 (ISO 8726)
- Continuous sinusoidal input ISO 7401
- Stopping distance at straight-line braking with ABS ISO 21994:2007
- Braking with split coefficient of friction ISO 14512
- Brake in a turn ISO 7975
- Power off reaction of a vehicle in a turn ISO 9816
- Acceleration 0-top speed
- Accelerating with split coefficient of friction
- Accelerating in a turn

3. Vehicle Model

The vehicle model that is considered to be used in this study is a 5+1 persons golf vehicle. The details of the vehicle properties are given in Figure 3(a). The reason for choosing this vehicle is to meet the service needs in large areas such as schools, hospitals and airports as an autonomous service vehicle.

Figure 3(b) shows the dynamic simulation model of this vehicle. Here, the study is carried out on a dual track vehicle model with 3 degrees of freedom. As seen in Figure 3(b) for the traction part, the vehicle is driven on the powertrain and wheel model. The traction force accelerates the vehicle body by overcoming the opposite force such as air friction, rolling and slope. It is represented from equation 1-4 [77].

$$m.\frac{dv_{veh}}{dt} = f_{veh} - (f_{rol} + f_{wind} + f_{grad}) \tag{1}$$

$$J_w.\frac{d\omega_w}{dt} = T_d - r_w.f_{veh} \tag{2}$$

$$T_d = \eta.T_m.n \tag{3}$$

$$T_m = P_{out}/\omega_m \tag{4}$$

The applied input torque is equal to the sum of the axle torque, braking torque and traction torque [77-81].

$$T_i = T_a - T_b + T_d \tag{5}$$

In the steering part, steering is carried out with the rack and pinion system. According to the driving scenario, the steering and traction parts are tried to be controlled with the control signals (Lateral (Yaw Rate) and Longitudinal (Reference Velocity)) produced by the driver. In this case, the transferred torque through the rack and pinion gear can be represented from equation 6 [82-83].

$$T_{sw} = -GK_m i + T_r + J_p a_p + c_p.\omega_m/G \tag{6}$$

The vehicle model shown in Figure 3 (a) uses DLGF 122200-4 of ABM company for traction. The rated specification of DLGF 122200-4 are 10 KWatt (KiloWatt), 20 Nm (Newton.meter) and 5000 RPM (Revolutions Per Minute). For steering, the vehicle model shown in Figure 3 (a) uses EPAS18 of DC Electronics company. The rated specification of EPAS18 are 0.45 KWatt, 34.5 Nm and 130 RPM.

Motor Power	10kW
Battery	8 x 6V, 11.5kWh
Max. Speed for Forward	25km/h
Max. Speed for Backward	8km/h
Range	80km (EU 134/2014)
Maximum Slope	%25
Charging Duration	%100 – 9h
Curb Weight	645kg
Passenger Capacity	1+5 Passengers
Transporting Capacity	600kg
Traction Capacity	1000kg
Tire Diameter	8.5inch
Vehicle Length	3240mm
Vehicle Width	1215mm
Unladen Height	1925mm
Ground Clearance	110mm
Wheelbase	2480mm

a) Specification of the Vehicle [75,77]

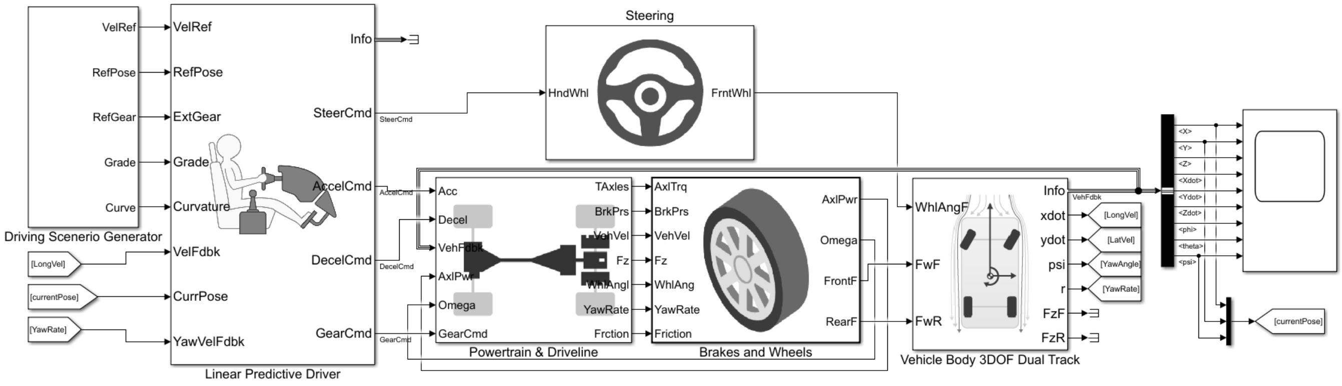

b) Dynamic Model of the Vehicle

Fig 3. Vehicle Model a) Specification of the Vehicle b) Dynamic Model of the Vehicle

4. Methodology

A generalized representation of the autonomous vehicle architecture is given in Figure 4. Since this study focuses on the traction and steering part, it is planned to carry out operations with the driving cycle in the traction part and with the driving scenario in the steering part. Therefore, the representation of the driving cycles and driving scenarios discussed is given in Figure 5.

As can be seen from Figure 5, the performed analyse~~i~~s in this study are dealt with two parts as traction and steering. Here, 3 different driving cycles are selected for traction. These are NEDC, US06 and WLTC Class 3 Low. Since the vehicle whose model is considered as a golf cart and it has a maximum of 25km/h, the 3 driving cycles are arranged to be evaluated on a similar time scale in accordance with the vehicle specification and adjusted according to the maximum speed.

On the other hand, Double Lane Change [84], Constant Radius

[85] and Slowly Increase Steer [86] are discussed in order to evaluate the maneuver for the steering part. Here, the driving scenarios are arranged similarly in accordance with both vehicle dynamics and maximum speed.

By running on both Driving Cycles and Driving Scenarios dynamic vehicle model, the parameters such as displacement, reference trajectory tracking, acceleration, yaw angle, tractive force, traction motor power-speed-torque, steering force, lateral displacement, lateral acceleration, steering motor power-speed-torque are dealt with and tried to be analyzed.

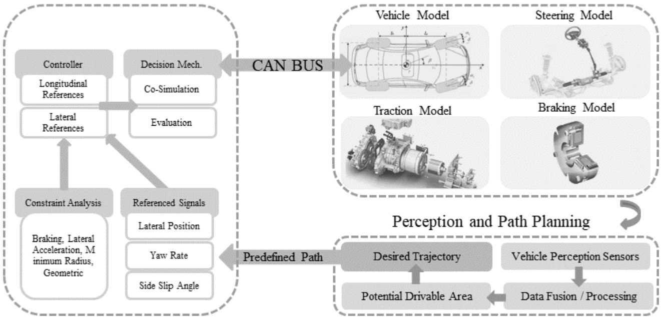

Fig 4. Generalized Autonomous Vehicle Architecture

A generalized representation of the autonomous vehicle architecture is given in Figure 4. Since this study focuses on the traction and steering part, it is planned to carry out operations with the driving cycle in the traction part and with the driving scenario in the steering part. Therefore, the representation of the driving cycles and driving scenarios discussed is given in Figure 5.

As can be seen from Figure 5, the performed analyse~~i~~s in this study are dealt with two parts as traction and steering. Here, 3 different driving cycles are selected for traction. These are NEDC, US06 and WLTC Class 3 Low. Since the vehicle whose model is considered as a golf cart and it has a maximum of 25km/h, the 3 driving cycles are arranged to be evaluated on a similar time scale in accordance with the vehicle specification and adjusted according to the maximum speed.

On the other hand, Double Lane Change [84], Constant Radius [85] and Slowly Increase Steer [86] are discussed in order to evaluate the maneuver for the steering part. Here, the driving scenarios are arranged similarly in accordance with both vehicle dynamics and maximum speed.

By running on both Driving Cycles and Driving Scenarios dynamic vehicle model, the parameters such as displacement, reference trajectory tracking, acceleration, yaw angle, tractive force, traction motor power-speed-torque, steering force, lateral displacement, lateral acceleration, steering motor power-speed-torque are dealt with and tried to be analyzed.

5. Results and Discussion

The main purpose of this study is to analyze the customized motor for autonomous electric vehicles that will work on a certain road profile for service purposes, instead of using the motor determined by overengineering as a result of traction and steering motor calculation. Therefore, in an autonomous electric vehicle, the selection of traction and steering motors with traditional calculations are compared and analyzed in driving cycles and scenarios.

For the traction analysis under NEDC, US06 and WLTC, the obtained results and the detailed information are shown in Figure 6. For the steering analysis under Double Lane Change, Constant Radius and Slowly Increase Steer, the obtained results and the detailed information are shown in Figure 7.

The obtained results from traction and steering analysis under the driving cycles and scenarios are summarized in Table 10 and Table 11. Here, the performance of traction and steering analyzes are evaluated relatively by 3 metrics to simplify the overall performances. For the traction, as shown in Table 10, WLTC forces the vehicle model to operate higher performance in comparison with NEDC and US06. On the other hand, for the steering analysis, CR and SIS force the vehicle model to operate higher performance in comparison with DLC.

Table 10. Traction Analysis under NEDC, US06 and WLTC

Traction Analysis	Displacement Error	MSE for Tracking	Max Acceleration	Lateral Deviation	Tractive Force	Motor Torque	Motor Speed	Motor Power	Overall Scores
NEDC	GOOD	GOOD	LOW	BETTER	HIGH	GOOD	GOOD	MID	GOOD
US06	BETTER	BETTER	HIGH	GOOD	LOW	GOOD	GOOD	LOW	BETTER
WLTC	GOOD	GOOD	HIGH	BEST	HIGH	GOOD	GOOD	HIGH	BEST

Table 11. Steering Analysis under DLC, CR and SIS

Steering Analysis	Correlation	Steering Force	Max Speed	Lateral Deviation	Lateral Acceleration	Motor Torque	Motor Speed	Motor Power	Overall Scores
DLC	BEST	LOW	MID	LOW	LOW	LOW	LOW	LOW	GOOD
CR	GOOD	MID	HIGH	HIGH	HIGH	MID	MID	MID	BEST
SIS	GOOD	HIGH	LOW	HIGH	MID	HIGH	HIGH	HIGH	BEST

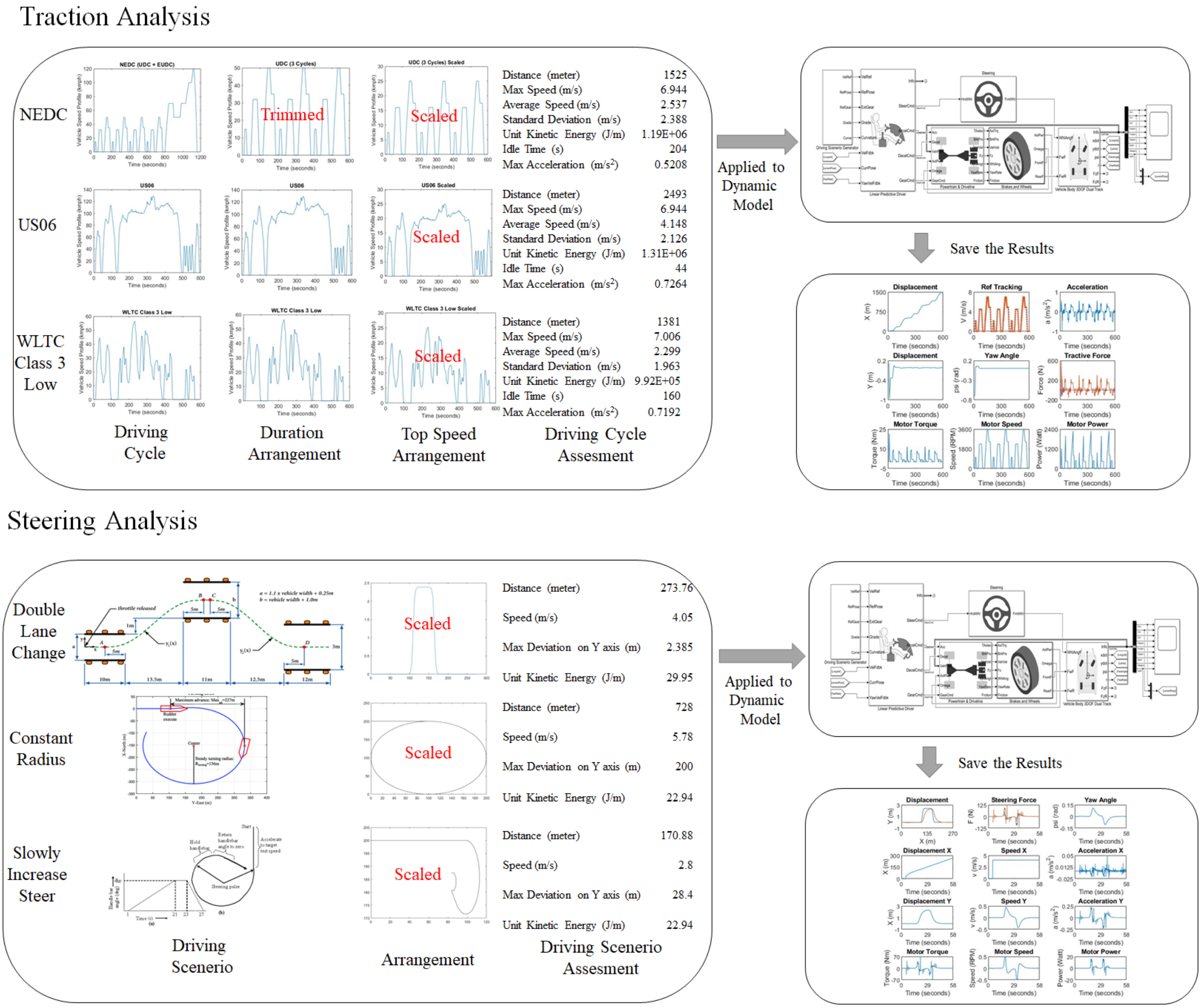

NEDC	
Distance (meter)	1525
Max Speed (m/s)	6.944
Average Speed (m/s)	2.537
Standard Deviation (m/s)	2.388
Unit Kinetic Energy (J/m)	1.19E+06
Idle Time (s)	204
Max Acceleration (m/s^2)	0.5208

US06	
Distance (meter)	2493
Max Speed (m/s)	6.944
Average Speed (m/s)	4.148
Standard Deviation (m/s)	2.126
Unit Kinetic Energy (J/m)	1.31E+06
Idle Time (s)	44
Max Acceleration (m/s^2)	0.7264

WLTC Class 3 Low	
Distance (meter)	1381
Max Speed (m/s)	7.006
Average Speed (m/s)	2.299
Standard Deviation (m/s)	1.963
Unit Kinetic Energy (J/m)	9.92E+05
Idle Time (s)	160
Max Acceleration (m/s^2)	0.7192

Double Lane Change	
Distance (meter)	273.76
Speed (m/s)	4.05
Max Deviation on Y axis (m)	2.385
Unit Kinetic Energy (J/m)	29.95

Constant Radius	
Distance (meter)	728
Speed (m/s)	5.78
Max Deviation on Y axis (m)	200
Unit Kinetic Energy (J/m)	22.94

Slowly Increase Steer	
Distance (meter)	170.88
Speed (m/s)	2.8
Max Deviation on Y axis (m)	28.4
Unit Kinetic Energy (J/m)	22.94

Fig 5. Methodology of Traction and Steering Analysis

Considering the obtained findings, it is necessary to compare the DLGF 122200-4 traction motor selected for the vehicle model and the demanded motor requirements during the driving cycles as torque-speed and power-speed for each driving cycle. Figure 8 shows the obtained results for the traction analysis. As can be seen from Figure 8, the demanded torque-speed-power is quite below the capacity of the DLGF 122200-4 traction motor. This clearly shows that the DLGF 122200-4 traction motor is an overengineering choice. Therefore, with an optimized and customized motor design, it is possible to gain from the design space by having a more compact structure. Besides, gains from power to weight ratio can provide increasing the range of electric vehicles by weight reduction

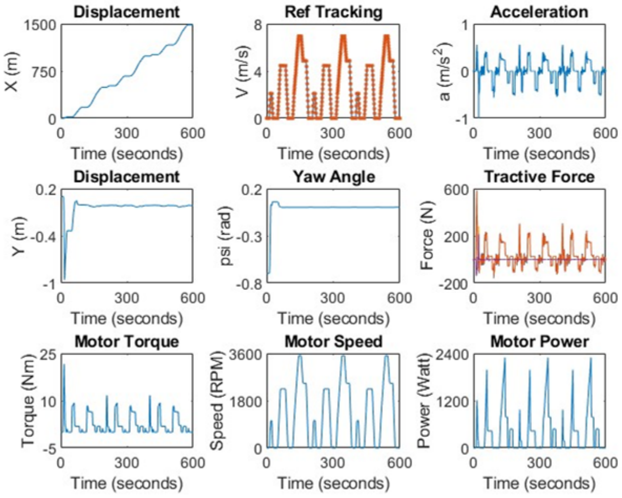

Displacement (X) (m)	
Total	1482.4
Expected	1525
Percentage Error	3%

Vehicle Speed (V) (m/s)	
Max Speed	6.9
Avg. Speed	2.4656
Std.Dev.	1.3456
MSE for Tracking	0.0186

Acceleration (a) (m/s^2)	
Deceleration	-1.0467
Max Acc.	0.5571
Avg. Acc.	-0.0017
Std.Dev.	0.1347

Displacement (Y) (m)	
Max	0.1
Min	-0.9578
Avg.	-0.0373
Std.Dev.	0.1142

Yaw Angle (psi) (rad)	
Max	0.0592
Min	-0.6982
Avg.	-0.0591
Std.Dev.	0.2068

Tractive Force (F) (N)	
Rear Right Max	563.041
Rear Left Max	583.118
Rear Right Avg	13.8467
Rear Left Avg	13.8525

Motor Torque (Nm)	
Max	21.6804
Min	0
Avg.	0.884
Std.Dev.	2.3978

Motor Speed (RPM)	
Max	3514
Min	-0.0718
Avg.	247.23
Std.Dev.	685.32

Motor Power (Watt)	
Max	2295.1
Min	-2.23E-04
Avg.	80.449
Std.Dev.	278.467

a) NEDC

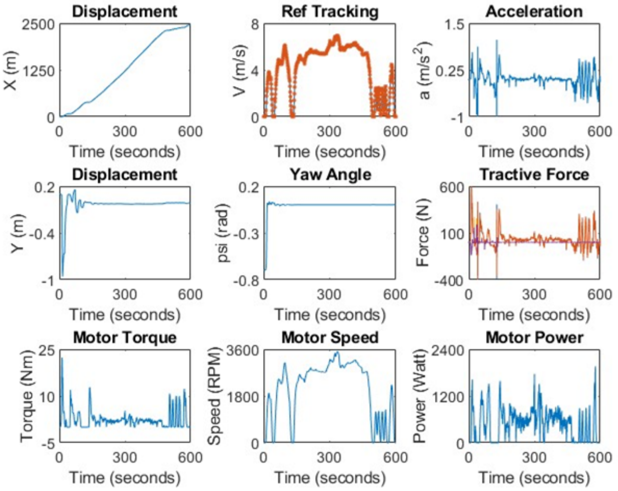

Displacement (X) (m)	
Total	2452.4
Expected	2493
Percentage Error	2%

Vehicle Speed (V) (m/s)	
Max Speed	6.8947
Avg. Speed	4.0801
Std.Dev.	1.44
MSE for Tracking	0.0109

Acceleration (a) (m/s^2)	
Deceleration	-1.4615
Max Acc.	1.0551
Avg. Acc.	-0.0011
Std.Dev.	0.0951

Displacement (Y) (m)	
Max	0.1585
Min	-0.9599
Avg.	0.0665
Std.Dev.	0.0676

Yaw Angle (psi) (rad)	
Max	0.0377
Min	-0.6981
Avg.	-0.0123
Std.Dev.	0.14

Tractive Force (F) (N)	
Rear Right Max	580.685
Rear Left Max	597.805
Rear Right Avg	8.217
Rear Left Avg	7.5003

Motor Torque (Nm)	
Max	22.31
Min	0
Avg.	0.4965
Std.Dev.	1.8953

Motor Speed (RPM)	
Max	3511
Min	-0.0718
Avg.	239.2
Std.Dev.	733.37

Motor Power (Watt)	
Max	1961
Min	-1.07E-04
Avg.	60.459
Std.Dev.	212.942

b) US06

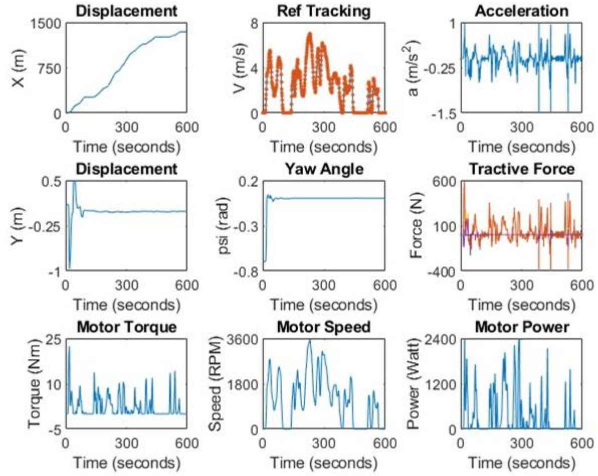

Displacement (X) (m)	
Total	1341.4
Expected	1381
Percentage Error	3%

Vehicle Speed (V) (m/s)	
Max Speed	6.9559
Avg. Speed	2.2314
Std.Dev.	1.2669
MSE for Tracking	0.0192

Acceleration (a) (m/s^2)	
Deceleration	-1.6531
Max Acc.	1.0342
Avg. Acc.	-0.001
Std.Dev.	0.132

Displacement (Y) (m)	
Max	0.5832
Min	-0.9653
Avg.	-0.0013
Std.Dev.	0.0746

Yaw Angle (psi) (rad)	
Max	0.0434
Min	-0.6982
Avg.	-0.0772
Std.Dev.	0.2201

Tractive Force (F) (N)	
Rear Right Max	582.713
Rear Left Max	587.874
Rear Right Avg	13.0069
Rear Left Avg	13.0071

Motor Torque (Nm)	
Max	22.406
Min	0
Avg.	0.8194
Std.Dev.	2.5081

Motor Speed (RPM)	
Max	3542
Min	-0.0718
Avg.	280.36
Std.Dev.	645.23

Motor Power (Watt)	
Max	2801.3
Min	-1.14E-04
Avg.	85.811
Std.Dev.	303.0285

c) WLTC

Fig 6. Driving Cycle Results for Traction

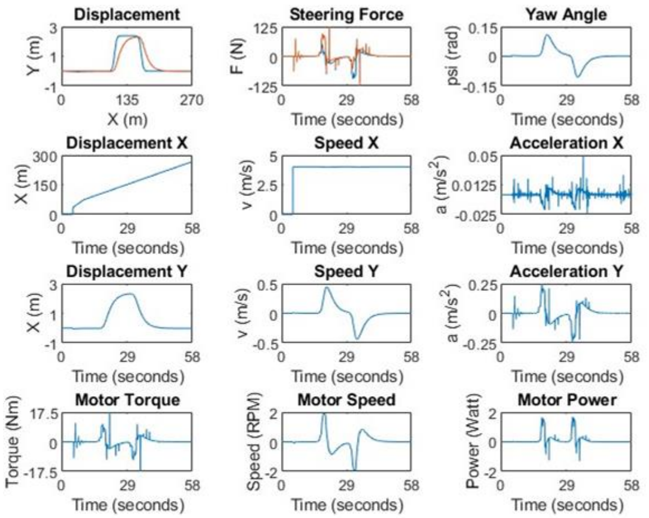

Displacement	
Correlation	79.71%

Steering Force (N)			
Left		Right	
Max	123.59	Max	127.97
Min	-131.71	Min	-127.11
Avg.	-2.87	Avg.	2.79
Std.Dev.	18.5	Std.Dev.	18.5

Yaw Angle (rad)	
Max	0.1097
Min	-0.1055
Avg.	0.0015
Std.Dev.	0.0377

Displacement X (m)	
Max	267.6
Min	0
Avg.	146.48
Std.Dev.	75.16

Speed X (m/s)	
Max	4.0162
Min	0
Avg.	3.66
Std.Dev.	1.12

Acceleration X (m/s^2)	
Max	0.0497
Min	-0.0287
Avg.	1.03E-06
Std.Dev.	0.004

Displacement Y (m)	
Max	2.315
Min	-0.0573
Avg.	0.5381
Std.Dev.	0.8461

Speed Y (m/s)	
Max	0.4421
Min	-0.4379
Avg.	3.28E-04
Std.Dev.	0.1526

Acceleration Y (m/s^2)	
Max	0.2505
Min	-0.2537
Avg.	-1.21E-04
Std.Dev.	0.0604

Motor Torque (Nm)	
Max	18.865
Min	-19.4125
Avg.	-0.00615
Std.Dev.	2.54

Motor Speed (RPM)	
Max	1.918
Min	-0.19444
Avg.	-1.34E-03
Std.Dev.	0.5424

Motor Power (Watt)	
Max	1.679
Min	-1.295
Avg.	0.11723
Std.Dev.	0.339

a) Double Lane Change (DLC)

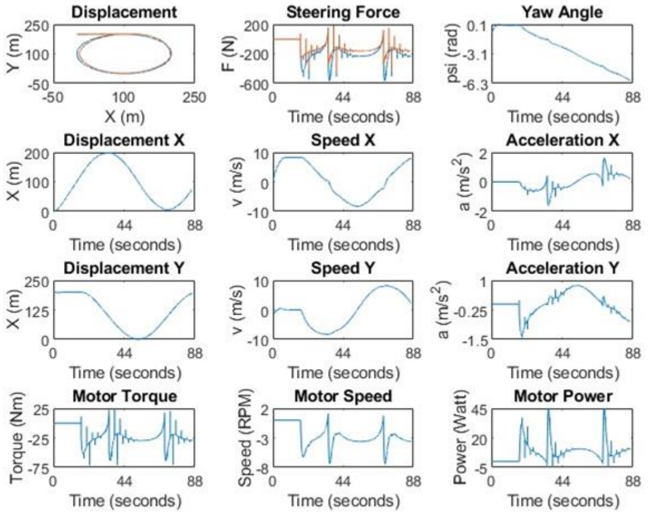

Displacement	
Correlation	76.36%

Steering Force (N)			
Left		Right	
Max	174.46	Max	183.94
Min	-570.53	Min	-44.63
Avg.	-162.38	Avg.	-110.58
Std.Dev.	128.05	Std.Dev.	77.9

Yaw Angle (rad)	
Max	0.0812
Min	-5.9952
Avg.	-2.3671
Std.Dev.	1.9259

Displacement X (m)	
Max	198.39
Min	0.1
Avg.	87.83
Std.Dev.	70.01

Speed X (m/s)	
Max	8.24
Min	-8.24
Avg.	0.9
Std.Dev.	5.7

Acceleration X (m/s^2)	
Max	1.6
Min	-1.6
Avg.	-3.60E-03
Std.Dev.	0.4859

Displacement Y (m)	
Max	200.13
Min	0.57
Avg.	119.75
Std.Dev.	74.24

Speed Y (m/s)	
Max	8.24
Min	-8.24
Avg.	-6.84E-02
Std.Dev.	5.34

Acceleration Y (m/s^2)	
Max	0.7975
Min	-1.4161
Avg.	2.39E-02
Std.Dev.	0.4591

Motor Torque (Nm)	
Max	26.88
Min	-71.455
Avg.	-20.4725
Std.Dev.	15.31

Motor Speed (RPM)	
Max	1.136
Min	-7.4116
Avg.	-2.4996
Std.Dev.	1.8036

Motor Power (Watt)	
Max	45.95
Min	-8.356
Avg.	7.765
Std.Dev.	8.519

b) Constant Radius (CR)

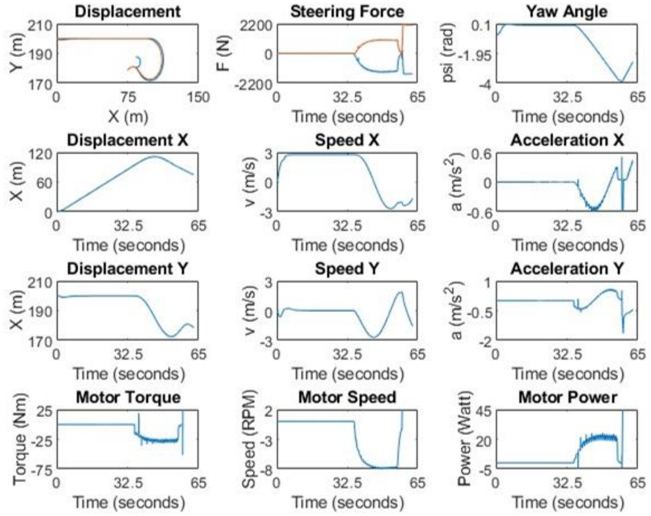

Displacement	
Correlation	82.99%

Steering Force (N)			
Left		Right	
Max	320.28	Max	2322
Min	-1531	Min	-302.17
Avg.	-472.3	Avg.	422.35
Std.Dev.	627.91	Std.Dev.	632.44

Yaw Angle (rad)	
Max	0.0732
Min	-3.8696
Avg.	-0.9435
Std.Dev.	1.3018

Displacement X (m)	
Max	111.32
Min	0.1
Avg.	64.25
Std.Dev.	37.04

Speed X (m/s)	
Max	2.76
Min	-2.69
Avg.	1.11
Std.Dev.	2.1

Acceleration X (m/s^2)	
Max	0.5058
Min	-0.6846
Avg.	-6.47E-02
Std.Dev.	0.1996

Displacement Y (m)	
Max	200.1
Min	172.46
Avg.	192.99
Std.Dev.	10.08

Speed Y (m/s)	
Max	1.88
Min	-2.7
Avg.	-3.36E-01
Std.Dev.	0.9973

Acceleration Y (m/s^2)	
Max	0.5975
Min	-1.667
Avg.	-2.80E-02
Std.Dev.	0.2964

Motor Torque (Nm)	
Max	23.615625
Min	-12.92375
Avg.	-0.93625
Std.Dev.	4.91125

Motor Speed (RPM)	
Max	12.068
Min	-8.008
Avg.	-1.3872
Std.Dev.	4.79

Motor Power (Watt)	
Max	107.5
Min	-9.349
Avg.	9.506
Std.Dev.	14.97

c) Slowly Increase Steer (SIS)

Fig 7. Driving Scenerio Results for Steering

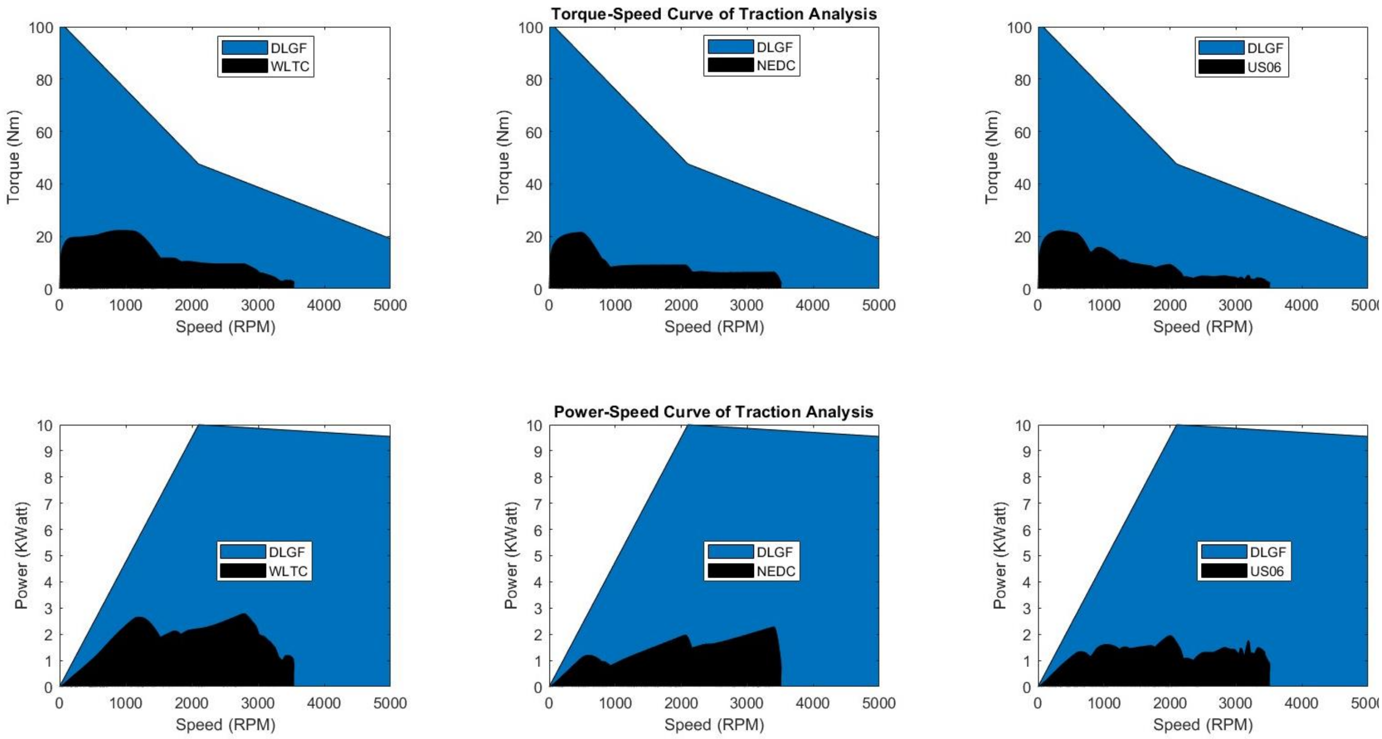

Fig 8. Traction Motor Analysis

Similarly, it is necessary to compare the EPAS18 steering motor selected for the vehicle model and the demanded torque-speed-power values in the driving scenarios for the steering analysis. Figure 9 shows the obtained findings for the steering analysis. As can be seen from Figure 9, it is observed that the demanded torque-speed-power is far below the capacity of the EPAS18, so it is an overengineering choice here as well. Although the power consumed on EPAS is very small, considering the electric vehicles and range problems, it is seen that a more efficient and compact design as a result of optimization will increase the efficiency.

6. Conclusions

In this study, the demands of the traction and steering requirements for an autonomous electric vehicle on a predetermined route to be followed within the scope of autonomous duty are tried to be evaluated. Considering autonomous vehicles, the main task is to provide lateral and longitudinal movements with traction and steering. Therefore, traction and steering motors are discussed here. In order to assess the traction part, the driving cycle is needed, and in order to assess the steering part, the driving scenario is needed. Within this scope, the studies in the literature are reviewed and the driving cycles and scenarios are analyzed. The potential driving cycle and driving scenarios are determined by taking into account the dynamics of the electric autonomous shuttle as a result of the evaluations. In order to obtain suitable driving cycles and driving scenarios for the specs of the vehicle, the parameters such as the maximum speed that the vehicle can reach and the driving cycles and driving scenarios are modified and arranged. The dynamic model of the vehicle is modeled in Matlab Simulink in accordance with the specs and it is made ready for analysis.

The parameters such as displacement, reference trajectory tracking, acceleration, yaw angle, tractive force, traction motor power-speed-torque, steering force, lateral displacement, lateral acceleration, steering motor power-speed are tried to be analyzed on the vehicle model running under driving cycles and scenarios such as NEDC, US06, WLTC, DLC, CR and SIS selected for Traction and Steering analysis. According to the analyzes, it is seen that the obtained results are at an acceptable level for trajectory tracking and other parameters.

On the other hand, it is observed that the traction and steering power-torque-speed values demanded by the dynamic vehicle model, which is run under driving cycles and driving scenarios, are far below the capacity of the DLGF traction motor selected for the vehicle with traditional methods and the EPAS18 steering motor, and an overengineering choice is made. It is seen that the autonomous service vehicle will work on a predetermined path and efficiency will increase with the selection of the optimal steering and traction motors, considering the range problem in electric vehicles.

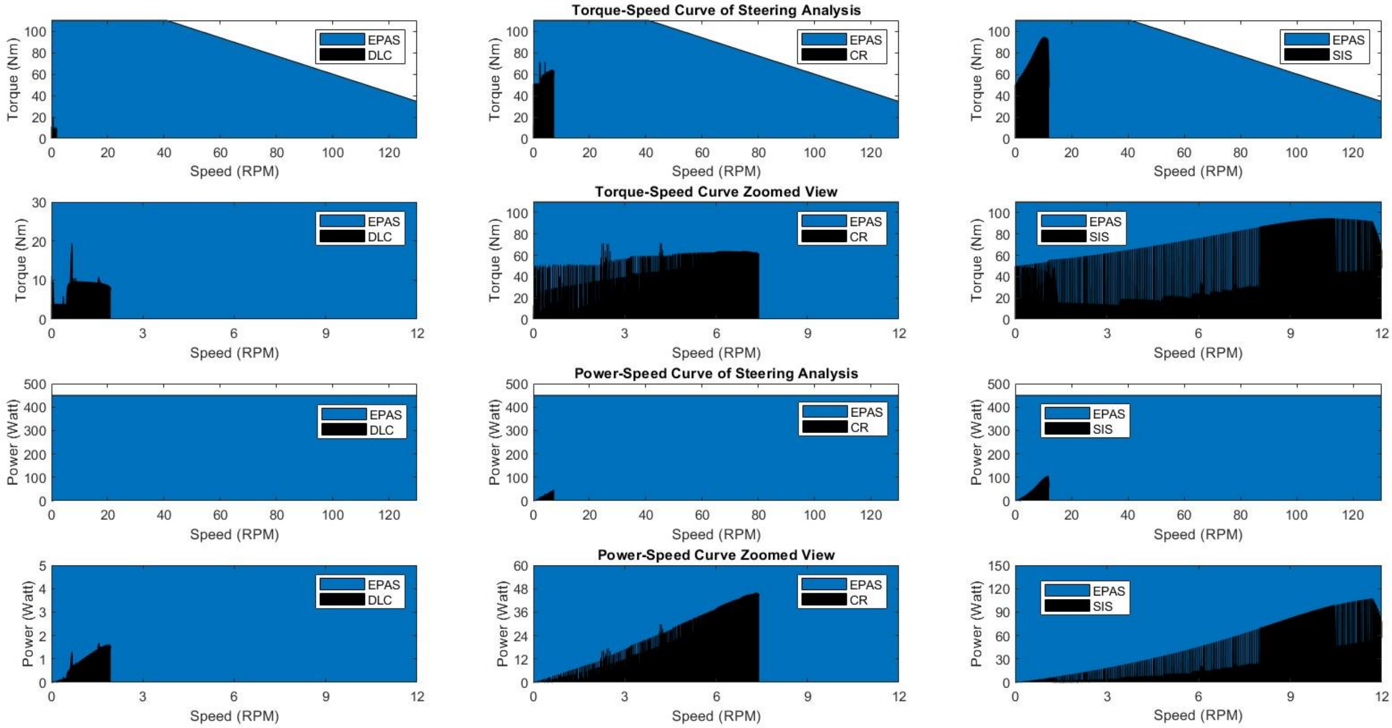

Torque-Speed Curve of Steering Analysis

Torque-Speed Curve Zoomed View

Power-Speed Curve of Steering Analysis

Power-Speed Curve Zoomed View

Fig 9. Steering Motor Analysis

Nomenclature

m : vehicle body mass (kg)
T_i : net input torque (Nm)
T_a : applied axle torque about wheel spin axis (Nm)
T_b : braking torque (Nm)
T_d : combined tire torque (Nm)
T_r : resistance torque (Nm)
T_m : torque from electric motor (Nm)
T_{sw} : steering wheel torque (Nm)
η : efficiency (%95)
n : transmission ratio (1:8)
G : transmission ratio (1:4)
a_p : angular acceleration of steering column (rad/s^2)
c_p : steering column damping (Nm.s/rad)
J_w : inertia of the wheel (kg.m^2)
J_p : rotary inertia of the steering column (kg.m^2)
P_{out} : motor output power (watt)
K_m : motor torque constant (Nm/Amp)
i : motor current (Amp)
ω_w, ω_m : wheel and rotor angular speed (rad/s)
ω_p : angular speed of the steering column (rad/s)
f_{veh} : traction force (N)
f_{rol} : rolling resistance (N)
f_{wind} : aerodynamic drag force (N)
f_{grad} : grading force (N)
v_{veh} : vehicle velocity (m/s)

Conflict of Interest Statement

The authors must declare that there is no conflict of interest in the study.

CRediT Author Statement

Uğur Demir: Conceptualization, Writing-original draft, Validation, Data curation, Formal analysis, **Zeliha Kamış Kocabıçak:** Conceptualization,

References

References

[1] Ehsani M., Gao Y, Emadi A. Modern Electric, Hybrid Electric, and Fuel Cell Vehicles - Fundamentals, Theory, and Design. CRC Press 2nd ed., Boca Raton, FL: Taylor and Francis Group, LLC. 2010.

[2] Demir U., Aküner M. C. Design and Analysis of Radiaxial Induction Motor. Electrical Engineering. 2018; 100(4): 2361-2371.

[3] Christensen, T., Sørensen, N.B., Bøg, B. Energy Efficient Control of an Induction Machine for an Electric Vehicle. Master Thesis, Aalborg University, Study Board of Industry and Global Business Development, Denmark. 2012.

[4] Demir U., Aküner M. C. Design and Optimization of in-Wheel Asynchronous Motor for Electric Vehicle. Journal of the Faculty of Engineering and Architecture of Gazi University. 2018; 18(2): 1-21.

[5] Emirler M. T., Uygan İ. M. C., Güvenç B. A., Güvenç L.Robust PID Steering Control in Parameter Space for Highly Automated Driving. International Journal of Vehicular Technology. 2014; 259465: 1687-5702.

[6] Ji J., Khajepour A., Melek W. W., Huang Y. Path Planning and Tracking for Vehicle Collision Avoidance Based on Model Predictive Control With Multiconstraints. IEEE Transactions on Vehicular Technology. 2017; 66(2): 952-964.

[7] Emirler M. T., Wang H., Güvenç B.A. Automated robust path following control based on calculation of lateral deviation and Yaw angle error. ASME 2015 dynamic systems and control conference, Columbus, OH, p.V003T50A009. New York: ASME. 2015.

[8] Demir U., Aküner M. C. Using Taguchi method in defining critical rotor pole data of LSPMSM considering the power factor and efficiency. Tehnički vjesnik. 2017; 24(2): 347- 353.

[9] Sun X., Shi Z., Lei G., Guo Y., Zhu J. Multi-Objective Design Optimization of an IPMSM Based on Multilevel Strategy. IEEE Transactions on Industrial Electronics. 2020; 68(1): 139-148.

[10] Bacha S., Saadi R., Ayad M.Y., Aboubou A. and Bahri M. A review on vehicle modeling and control technics used for autonomous vehicle path following. 2017 International Conference on Green Energy Conversion Systems (GECS). 2017; 1-6.

[11] Guvenc B. A., Guvenc L. Robust two degree-of-freedom add-on controller design for automatic steering. IEEE Transactions on Control Systems Technology. 2002; 10(1): 137-148.

[12] Kocakulak T., Solmaz, H. Ön ve son iletimli paralel hibrit araçların bulanık mantık yöntemi ile kontrolü ve diğer güç sistemleri ile karşılaştırılması. Gazi Üniversitesi Mühendislik Mimarlık Fakültesi Dergisi. 2020; 35(4): 2269-2286.

[13] Snider J. M. Automatic Steering Methods for Autonomous Automobile Path Tracking. Master Thesis, Robotics Institute, Carnegie Mellon University, Pittsburgh, Pennsylvania. 2009.

[14] Li L., Chaosheng H., Minghui L., Shuming S. Study on the combined design method of transient driving cycles for passenger car in Changchun. 2008 IEEE Vehicle Power and Propulsion Conference. 2008; 1-5.

[15] Zhuang J. H., Xie H.,Yan Y. Remote self-learning of driving cycle for electric vehicle demonstrating area. 2008 IEEE Vehicle Power and Propulsion Conference. 2008; 1-4.

[16] Liang Z. Xin Z., Yi T., Xinn Z. Intelligent Energy Management Based on the Driving Cycle Sensitivity Identification Using SVM. 2009 Second International Symposium on Computational Intelligence and Design. 2009; 513-516.

[17] Yi T., Xin Z., Liang Z., Xinn, Z. Intelligent Energy Management Based on Driving Cycle Identification Using Fuzzy Neural Network. 2009 Second International Symposium on Computational Intelligence and Design. 2009; 501-504.

[18] Shiqi O., Yafu Z., Jing L., Pu J., Baoyu T. Development of hybrid city bus's driving cycle. 2011 International Conference on Electric Information and Control Engineering. 2011; 2112-2116.

[19] Zhuang J., Xie H., Li S., Yan Y., Zhu Z. Remote self-learning of driving cycle for hybrid electric vehicle. 2011 International Conference on Electrical and Control Engineering. 2011; 4029-4032.

[20] Liu L., Huang C., Lu B., Shi S., Zhang Y., Cheng J. Study on the design method of time-variant driving cycles for EV based on Markov Process. 2012 IEEE Vehicle Power and Propulsion Conference. 2012; 1277-1281.

[21] Chrenko D., Garcia Diez I., Le Moyne L. Artificial driving cycles for the evaluation of energetic needs of electric vehicles. 2012 IEEE Transportation Electrification Conference and Expo (ITEC). 2012; 1-5.

[22] Ma X., Ming W. Energy-saving driving mode for PHEV drivers based on energy cycle model. IET Hybrid and Electric Vehicles Conference 2013 (HEVC 2013). 2013; 1-5.

[23] Schwarzer V., Ghorbani R. Drive Cycle Generation for Design Optimization of Electric Vehicles. IEEE Transactions on Vehicular Technology. 2013; 62(1): 89-97.

[24] Shi S., et al. Research on Markov Property Analysis of Driving Cycle. 2013 IEEE Vehicle Power and Propulsion Conference (VPPC). 2013; 1-5.

[25] Asus, Z., Aglzim, E., Chrenko D., Daud Z. C., Le Moyne L. Dynamic Modeling and Driving Cycle Prediction for a Racing Series Hybrid Car. IEEE Journal of Emerging and Selected Topics in Power Electronics. 2014; 2(3): 541-551.

[26] Xing J., Han X., Ye H., Cui Y., Ye, H. Driving cycle recognition for hybrid electric vehicle. 2014 IEEE Conference and Expo Transportation Electrification Asia-Pacific (ITEC Asia-Pacific). 2014; 1-6.

[27] Zhang B., Gao X., Xiong X., Wang X., Yang H. Development of the Driving Cycle for Dalian City. 2014 8th International Conference on Future Generation Communication and Networking. 2014; 60-63.

[28] Nejad A. Z., Deilami S., Masoum M. A. S., Haghdadi N. Map-based linear estimation of drive cycle for hybrid electric vehicles. 2015 Australasian Universities Power Engineering Conference (AUPEC). 2015; 1-5.

[29] Nyberg P., Frisk E., Nielsen, L. Using Real-World Driving Databases to Generate Driving Cycles With Equivalence Properties. IEEE Transactions on Vehicular Technology. 2016; 65(6): 4095-4105.

[30] Divakarla K. P., Emadi A., Razavi, S. N. Journey Mapping—A New Approach for Defining Automotive Drive Cycles. IEEE Transactions on Industry Applications. 2016; 52(6): 5121-5129.

[31] Sun B. Driving cycle construction methodology based on Markov process and uniform distribution. 2016 35th Chinese Control Conference (CCC). 2016; 9300-9304.

[32] Chen Z., Li L. Yan B., Yang C., Marina Martínez C., Cao D. Multimode Energy Management for Plug-In Hybrid Electric Buses Based on Driving Cycles Prediction. IEEE Transactions on Intelligent Transportation Systems. 2016; 17(10): 2811-2821.

[33] Silvas E., Hereijgers K., Peng H., Hofman T., Steinbuch M. Synthesis of Realistic Driving Cycles With High Accuracy and Computational Speed, Including Slope Information. IEEE Transactions on Vehicular Technology. 2016; 65(6): 4118-4128.

[34] Liessner R., Dietermann A. M., Bäker B., Lüpkes K.Derivation of real-world driving cycles corresponding to traffic situation and driving style on the basis of Markov models and cluster analyses. 6th Hybrid and Electric Vehicles Conference (HEVC 2016). 2016; 1-7.

[35] Wang Y., Zhang N., Xia J., Liu B., Wu Y. An Intelligent Identification Method of Vehicle Driving Cycle Based on LVQ Model. 2017 10th International Symposium on Computational Intelligence and Design (ISCID). 2017; 240-243.

[36] Mahayadin A. R., et al. Development of Driving Cycle Construction Methodology in Malaysia's Urban Road System. 2018 International Conference on Computational Approach in Smart Systems Design and Applications (ICASSDA). 2018; 1-5.

[37] Zhang M., Shi S., Lin N., Yue B. High-Efficiency Driving Cycle

Generation Using a Markov Chain Evolution Algorithm. IEEE Transactions on Vehicular Technology. 2019; 68(2): 1288-1301.

[38] Sun R., Tian Y., Zhang H., Yue R., Lv B., Chen J. Data-Driven Synthetic Optimization Method for Driving Cycle Development. IEEE Access. 2019; 7: 162559-162570.

[39] Kharrazi S., Almén M., Frisk E., Nielsen L. Extending Behavioral Models to Generate Mission-Based Driving Cycles for Data-Driven Vehicle Development. IEEE Transactions on Vehicular Technology. 2019; 68(2): 1222-1230.

[40] Wasserburger A., Hametner C. Automated Generation of Real Driving Emissions Compliant Drive Cycles Using Conditional Probability Modeling. 2020 IEEE Vehicle Power and Propulsion Conference (VPPC). 2020; 1-6.

[41] Förster D., Inderka R. B., Gauterin F. Data-Driven Identification of Characteristic Real-Driving Cycles Based on k-Means Clustering and Mixed-Integer Optimization. IEEE Transactions on Vehicular Technology. 2020; 69(3): 2398-2410.

[42] Shi S., Zhang M., Lin N., Yue B. Low-Cost Reconstruction of Typical Driving Cycles Based on Empirical Information and Low-Frequency Speed Data. IEEE Transactions on Vehicular Technology. 2020; 69(8): 8221-8231.

[43] Zhang M., Cheng W., Shen Y. Designing Heavy-Duty Vehicles' Four-Parameter Driving Cycles to Best Represent Engine Distribution Consistency. IEEE Access. 2020; 8: 212079-212093.

[44] Staackmann M., Liaw B. Y., Yun D. Y. Y. Dynamic driving cycle analyses using electric vehicle time-series data. IECEC-97 Proceedings of the Thirty-Second Intersociety Energy Conversion Engineering Conference. 1997; 2014-2018.

[45] Naylor S. M., Pickert V., Atkinson D. J. Fuel Cell Drive Train Systems -- Driving Cycle Evaluation of Potential Topologies. 2006 IEEE Vehicle Power and Propulsion Conference. 2006; 1-6.

[46] Fan J., et al.Thermal Analysis of Permanent Magnet Motor for the Electric Vehicle Application Considering Driving Duty Cycle. IEEE Transactions on Magnetics. 2010; 46(6): 2493-2496.

[47] Chu L., Yin J., Yao L., Wang W. The method for matching the PMSM's base parameters of the Hybrid Electric Vehicle based on drive cycle. Proceedings of 2011 International Conference on Electronic & Mechanical Engineering and Information Technology. 2011; 3234-3237.

[48] Li J., Wang W., Liu G., Lu F. Simulation and emission experiment of Changan hybrid electric vehicle (HEV) under the Instable drive cycle conditions. 2011 International Conference on Electric Information and Control Engineering. 2011; 2578-2581.

[49] Rothe R., Hameyer K. Life expectancy calculation for electric vehicle traction motors regarding dynamic temperature and driving cycles. 2011 IEEE International Electric Machines & Drives Conference (IEMDC). 2011; 1306-1309.

[50] Juris P., Brune A.,Ponick B. A coupled thermal-electromagnetic energy consumption calculation for an electric vehicle with wheel hub drive considering different driving cycles. 2012 IEEE Vehicle Power and Propulsion Conference. 2012; 28-31.

[51] Chen L., Wang J., Lazari P., Xiao C. Optimizations of a permanent magnet machine targeting different driving cycles for electric vehicles. 2013 International Electric Machines & Drives Conference. 2013; 855-862.

[52] Wu X., Jiang T., Du J., Hu C. Comparison of different driving cycles control effects of an extended-range electric bus. Proceedings of 2013 2nd International Conference on Measurement, Information and Control. 2013; 1073-1076.

[53] Lintern M. A., Chen R., Carroll S., Walsh C. Simulation study on the measured difference in fuel consumption between real-world driving and ECE-15 of a hybrid electric vehicle. IET Hybrid and Electric Vehicles Conference (HEVC 2013). 2013; 1-6.

[54] Sridharan S., Krein P. T. Induction motor drive design for traction application based on drive-cycle energy minimization. 2014 IEEE Applied Power Electronics Conference and Exposition - APEC 2014. 2014; 1517-1521.

[55] Yingnan W., Zhu W., Schaefer U. Study on the real time driving cycles and its influence on design of the electrical motor of EV. 2014 IEEE Conference and Expo Transportation Electrification Asia-Pacific (ITEC Asia-Pacific). 2014; 1-6.

[56] Patel V.I., Wang J., Wang W., Chen X. Thermal design and analysis of 6-phase fractional slot permanent magnet machines considering driving cycles. 7th IET International Conference on Power Electronics, Machines and Drives (PEMD). 2014;1-6.

[57] Günther S., Ulbrich S., Hofmann W. Driving cycle-based design optimization of interior permanent magnet synchronous motor drives for electric vehicle application. 2014 International Symposium on Power Electronics, Electrical Drives, Automation and Motion. 2014; 25-30.

[58] Boscaino V., Miceli R. Analysis of driving cycles effects on power supply requirements of a fuel cell powered light-weight electric vehicle. 2015 IEEE International Electric Machines & Drives Conference (IEMDC), 2015; 853-859.

[59] Carraro E., Morandin M., Bianchi N. Traction PMASR Motor Optimization According to a Given Driving Cycle. in IEEE Transactions on Industry Applications. 2016; 52(1): 209-216.

[60] Arfa Grunditz E., Thiringer T. Characterizing BEV Powertrain Energy Consumption, Efficiency, and Range During Official and Drive Cycles From Gothenburg, Sweden. IEEE Transactions on Vehicular Technology. 2016; 65(6,): 3964-3980.

[61] Fen G., Fei Z. A study of driving cycle for electric cars on Beijing urban and suburban roads. 2016 IEEE International Conference on Power and Renewable Energy (ICPRE). 2016; 319-322.

[62] Degrenne N., Mollov S. Real-life vs. standard driving cycles and implications on EV power electronic reliability. IECON 2016 - 42nd Annual Conference of the IEEE Industrial Electronics Society. 2016; 2177-2182.

[63] Li Q., Fan T., Wen X., Li Y., Wang Z., Guo J. Design optimization of interior permanent magnet sychronous machines for traction application over a given driving cycle. IECON 2017 - 43rd Annual Conference of the IEEE Industrial Electronics Society. 2017; 1900-1904.

[64] Kitzberger M., Bramerdorfer G., Silber S., Mitterhofer H., Amrhein W. Influence of Hysteresis and Eddy Current Losses on Electric Drive Energy Balance in Driving Cycle Operation,. 2018 8th International Electric Drives Production Conference (EDPC). 2018; 1-7.

[65] Charadsuksawat A., Laoonual Y., Chollacoop N. Comparative Study of Hybrid Electric Vehicle and Conventional Vehicle Under New European Driving Cycle and Bangkok Driving Cycle. 2018

IEEE Transportation Electrification Conference and Expo, Asia-Pacific (ITEC Asia-Pacific). 2018; 1-6.

[66] Tan D., Xue H., Yang K., Li A., Wang H. Study on the Thermal Characteristics of In-Wheel Motor Drive System Based on Driving Cycles. IEEE Access. 2019; 7: 14463-14471.

[67] Tian L. Wu L., Huang X., Fang Y.Driving range parametric analysis of electric vehicles driven by interior permanent magnet motors considering driving cycles. CES Transactions on Electrical Machines and Systems. 2019; 3(4): 377-381.

[68] Lekshmi S., Lal P. P. S. Range Extension of Electric Vehicles with Independently Driven Front and Rear PMSM Drives by Optimal Driving and Braking Torque Distribution. 2020 IEEE International Conference on Power Electronics, Smart Grid and Renewable Energy (PESGRE2020). 2020; 1-6.

[69] Vignesh S., Bhateshvar Y. K., Agrewale M. R. B., Vora K. C. Significance of Driving Cycle on Performance Parameters and Range in Small Electric Vehicle. 2020 IEEE First International Conference on Smart Technologies for Power, Energy and Control (STPEC). 2020; 1-5.

[70] Sun X., Shi Z., Cai Y., Lei G., Guo Y., Zhu J. Driving-Cycle-Oriented Design Optimization of a Permanent Magnet Hub Motor Drive System for a Four-Wheel-Drive Electric Vehicle. IEEE Transactions on Transportation Electrification. 2020; 6(3): 1115-1125.

[71] Sarathkumar T. V., Poornanand M., Goswami A. K. Modelling and Simulation of Electric Vehicle Drive Through SAEJ227 & EUDC Cycles. 2020 IEEE Students Conference on Engineering & Systems (SCES). 2020; 1-5.

[72] Diao K., Sun X., Lei G., Bramerdorfer G., Guo Y., Zhu J. System-Level Robust Design Optimization of a Switched Reluctance Motor Drive System Considering Multiple Driving Cycles. IEEE Transactions on Energy Conversion. 2021; 36(1): 348-357.

[73] Demir U., Kocabıcak Z. K. Performance assessments of the material for the traction motor cores of an electric racing kart. Material Testing. 2021; 63(6): 519-528.

[74] Bagheri M., Farjah E., Ghanbari T. Selective Utilized Phase Number of Multiphase Induction Motors Strategy to Enhance Electric Vehicles' Drive Range. 12th Power Electronics, Drive Systems, and Technologies Conference (PEDSTC). 2021; 1-5.

[75] Demir U. Improvement of the power to weight ratio for an induction traction motor using design of experiment on neural network. Electr Eng. 2021; 103: 2267–2284.

[76] Karlsson A. Test Procedures and Evaluation Tools for Passenger Vehicle Dynamics. Master Thesis, Chalmers University of Technology. 2014.

[77] Demir U. IM to IPM design transformation using neural network and DoE approach considering the efficiency and range extension of an electric vehicle. Electr Eng. 2022; 104: 1141–1152.

[78] Gillespie T. Fundamentals of Vehicle Dynamics. Warrendale, PA: Society of Automotive Engineers (SAE). 1992.

[79] Besselink I.J.M., Schmeitz A.J.C., Pacejka, H. B. An improved Magic Formula/Swift tyre model that can handle inflation pressure changes. Vehicle System Dynamics: International Journal of Vehicle Mechanics and Mobility. 2010; 48(1): 42-3114.

[80] Pacejka, H. B. Tire and Vehicle Dynamics. United Kingdom: SAE and Butterworth-Heinemann, 3rd ed. Oxford. 2012.

[81] Schmid S. R., Hamrock B. J., Jacobson B. O. Fundamentals of Machine Elements. Boca Raton: CRC Press 3rd ed. 2014.

[82] Kim S. H., Chu C. N. A new manual steering torque estimation model for steer-by-wire systems. Proc IMechE Part D: J Automobile Engineering. 2016; 230 (7): 993-1008.

[83] Na S., Li Z., Quiu F., Zhang C. Torque control of electric power steering system based on improved active disturbance rejection control. Mathematical Problems in Engineering. 2020; 6509607: 13.

[84] Jalali, K., Uchida, T., McPhee, J., Lambert, S. Development of an Advanced Fuzzy Active Steering Controller and a Novel Method to Tune the Fuzzy Controller. SAE Int. J. Passeng. Cars – Electron. Electr. Syst. 2013; 6: 241–254.

[85] Shuai Y., Li G., Xu J., Zhang H. An Effective Ship Control Strategy for Collision-Free Maneuver Toward a Dock. IEEE Access. 2020; 8: 110140-110152.

[86] Mukherjee S., Mohan D., Gawade, T.R. Three-wheeled scooter taxi: A safety analysis. Sadhana. 2007; 32: 459–478.